

Prospects for Very High Energy Blazar Survey by the Next Generation Cherenkov Telescopes

Yoshiyuki Inoue¹, Tomonori Totani¹, & Masaki Mori²

¹*Department of Astronomy, Kyoto University, Kitashirakawa, Sakyo-ku, Kyoto 606-8502, Japan*

²*Department of Physics, Ritsumeikan University, 1-1-1 Noji Higashi, Kusatsu, Shiga 525-8577, Japan*
inoue@kustastro.kyoto-u.ac.jp

(Received (reception date); accepted (acceptation date))

Abstract

The prospects for future blazar surveys by next-generation very high energy (VHE) gamma-ray telescopes, such as Advanced Gamma-ray Imaging System (AGIS) and Cherenkov Telescope Array (CTA), are investigated using the latest model of blazar luminosity function and its evolution which is in good agreement with the flux and redshift distribution of observed blazars as well as the extragalactic gamma-ray background. We extend and improve the template of spectral energy distributions (SEDs) based on the blazar SED sequence paradigm, to make it reliable also in the VHE bands (above 100 GeV) by comparing with the existing VHE blazar data. Assuming the planned CTA sensitivities, a blind survey using a total survey time of ~ 100 hrs could detect ~ 3 VHE blazars, with larger expected numbers for wider/shallower surveys. We also discuss following-up of *Fermi* blazars. Detectability of VHE blazars in the plane of *Fermi* flux and redshift is presented, which would be useful for future survey planning. Prospects and strategies are discussed to constrain the extragalactic background light (EBL) by using the absorption feature of brightest blazar spectra, as well as cut-offs in the redshift distribution. We will be able to get useful constraints on EBL by VHE blazars at different redshifts ranging 0.3–1 TeV corresponding to $z = 0.10$ –0.36.

Key words: galaxies : active – galaxies : jet – gamma rays : theory

1. Introduction

Very high energy (VHE; above 100 GeV) gamma-ray astronomy has now firmly been established by the observations of the state-of-the-art imaging atmospheric Cherenkov Telescopes (IACTs) such as H.E.S.S., MAGIC, and VERITAS (see de Angelis, Mansutti, & Persic 2008; Mori 2009, for reviews). Further progress is anticipated in the near future by the planned next-generation IACTs such as Cherenkov Telescope Array (CTA) and Advanced Gamma-ray Imaging System (AGIS). The sensitivities of all-sky monitoring VHE gamma-ray experiments are also expected to improve by the future projects such as the High Altitude Water Cherenkov Experiment (HAWC) and the Tibet-III/MD experiment.

Current IACTs have already found ~ 100 VHE sources including ~ 25 blazars. Blazars, a class of active galactic nuclei (AGNs), are the dominant population in the extragalactic gamma-ray sky. Almost all of the extragalactic sources detected by EGRET (Energetic Gamma-Ray Experiment Telescope) on board the Compton Gamma Ray Observatory are blazars (Hartman et al. 1999). Moreover, 3 months bright source and 11 months catalog by the *Fermi* gamma-ray space telescope (*Fermi*) have recently also showed that most of the extragalactic sources are blazars (Abdo et al. 2009a, 2009c, 2010), and we expect that more than 1000 blazars will be detected by *Fermi* in the near future (e.g. Narumoto & Totani 2006; Dermer 2007; Inoue & Totani 2009). The number of VHE blazars are expected to dramatically increase with the improved next-generation IACT sensitivity. Therefore, it would be possible to do a statistical study of VHE blazars in the CTA/AGIS era, which would provide a crucial key to under-

stand AGN populations and high energy phenomena around super massive black holes in AGNs and jets.

The purpose of this paper is to study the prospect of future blazar surveys by IACTs, especially for the statistical power of future VHE blazar sample that can be obtained by realistic observing time of next-generation IACTs. For this purpose, blazar gamma-ray luminosity function (GLF) and spectral energy distribution (SED) are needed. The blazar GLF has been studied in detail by many papers (Padovani et al. 1993; Stecker, Salamon, & Malkan 1993; Salamon & Stecker 1994; Chiang et al. 1995; Stecker & Salamon 1996; Chiang & Mukherjee 1998; Mücke & Pohl 2000; Narumoto & Totani 2006; Dermer 2007; Inoue & Totani 2009). Inoue & Totani (2009) (hereafter IT09) has recently presented a new blazar GLF taking into account the blazar SED sequence (see §2.1), which is in nice agreement with the CGRO/EGRET and *Fermi*/LAT data. We utilize this IT09 model to predict the expected number and distributions of physical quantities of VHE blazars in future IACT surveys. Since the SED model of IT09 was constrained only at the photon energies under GeV, we construct a new blazar SED template by modifying that used in IT09 in accordance with the available VHE blazar data. By using our updated blazar sequence and GLF model, it is possible for us to make predictions for future VHE gamma-ray observations, which is the most reliable based on available observed data.

Extragalactic background light (EBL) in the optical and infrared bands contains the information about the history of star formation activity in the universe, and knowing EBL quantitatively is an important step to understand galaxy formation in the cosmological context. However, it is hard to measure EBL spectrum directly, mainly because of the difficulty in sub-

tracting foreground emission (see Hauser & Dwek 2001, for reviews). VHE observations provide a completely independent constraint on EBL, since VHE gamma-ray photons propagating the universe are absorbed via electron-positron pair creation with the EBL photons (Gould & Schröder 1966; Jelley 1966). Some useful limits have already been obtained by VHE blazar observations (Aharonian et al. 2006a; MAGIC Collaboration, Albert, et al. 2008), up to the redshift of $z = 0.536$ by using 3C279 data. The next generation IACTs will shed further light on this issue, and we discuss the prospect about this as a particular application of our study.

This paper is organized as follows. We introduce our updated blazar SED template and GLF model, as well as the model of VHE gamma-ray absorptions by EBL in §2. In §3, we make predictions for the expected number and statistics of future VHE blazar surveys assuming some observing modes. We discuss the prospect for the determination of EBL by VHE blazars in §4. Summary is given in §5. Throughout this paper, we adopt the standard cosmological parameters of $(h, \Omega_M, \Omega_\Lambda) = (0.7, 0.3, 0.7)$.

2. Model Description

2.1. Blazar Gamma-ray Spectrum and Luminosity Function

IT09 has recently developed a blazar GLF model based on the latest determination of X-ray luminosity function of AGNs (Ueda et al. 2003; Hasinger, Miyaji, & Schmidt 2005), featuring so called luminosity dependent density evolution (LDDE). Another new feature of IT09 is taking into account the blazar SED sequence. Blazar sequence is a feature seen in the mean SED of blazars that the synchrotron and inverse Compton (IC) peak photon energies decrease as the bolometric luminosity increases [Fossati et al. (1997); Kubo et al. (1998); Fossati et al. (1998); Donato et al. (2001); Ghisellini, Maraschi, & Tavecchio (2009), but see also Padovani et al. (2007)]. The key parameters in GLF have carefully been determined to match the observed flux and redshift distribution of EGRET blazars by a likelihood analysis. Recently, the predicted extragalactic gamma-ray background (EGRB) spectrum by IT09 including non-blazar AGNs contributing to MeV bands (Inoue, Totani, & Ueda 2008) has been found to be in excellent agreement with the new determination of the EGRB spectrum reported by *Fermi* (Fermi-LAT collaboration 2010; Inoue et al. 2010).

The gamma-ray SED of the blazar sequence model used in IT09 is constrained only by the EGRET data whose energy range is 30 MeV – 30 GeV. Figs. 1 and 2 show multi-wavelength SEDs and radio-to-gamma-ray luminosity relation of VHE blazars, respectively. To avoid the absorption effect by EBL at high redshift, we have selected 12 VHE blazars below $z = 0.14$ where optical depth for 1 TeV photon is $\lesssim 1$. We have obtained SED data from published papers for VHE gamma-ray data (see the caption of Fig. 1) and from the NASA/IPAC Extragalactic Database (NED) for other wavelength data¹. By comparing with the observed data of VHE blazars, we have updated our blazar SED sequence model to properly reproduce typical VHE flux of observed blazars. A source of systematic

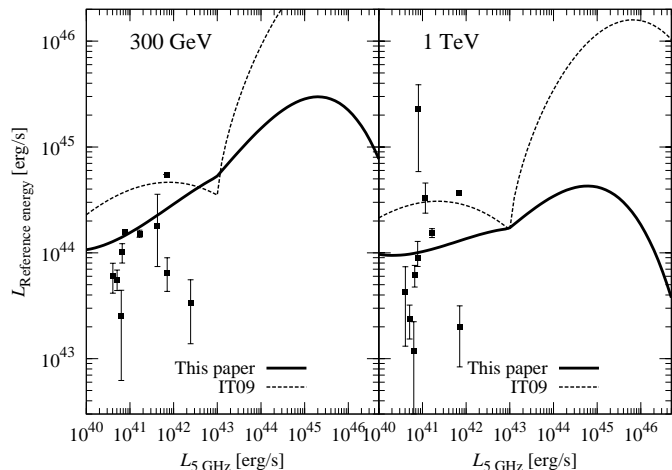


Fig. 2. Gamma-ray and 5GHz radio luminosity relations in νL_ν . The VHE luminosities in the left and right panels are at 300 GeV and 1 TeV, respectively. Data points are the same as those of 12 blazars in Fig. 1, except for H 1426+428 and 1ES 0229+200 in the left panel, and the BL Lac and 1ES 0806+524 in the right panel, because of non-detections in the corresponding energy bands. Gamma-ray luminosity is deabsorbed using the optical depth model of Totani & Takeuchi (2002) for intergalactic absorption. Solid and dashed curves correspond to the blazar sequence models by this paper and IT09, respectively.

uncertainty in this procedure is the variability of blazars; generally blazars show rapid and violent variability, and hence it is difficult to accurately estimate the VHE luminosity averaged over a long time. Here we simply collected published VHE flux data in the literature, except for those of observations aiming at blazars during flares.

As shown in Figs. 1 and 2, the sequence model of IT09 tends to overestimate VHE luminosity, but the new formulation reproduces a rough mean of VHE luminosities, though there is still significant scatter around the mean. Furthermore, the IT09 model shows a kink in the radio-VHE gamma-ray luminosity correlation, because of a mathematical problem of the connection between different luminosity ranges. This kink has also been removed in the new formulation. The new formulation of our updated blazar SED sequence templates is presented in Appendix in detail. We use this sequence template as the best model currently available to predict the statistics of VHE blazars based on the luminosity function determined at lower photon energy bands. Our SED template is also consistent with very recent MAGIC stacking analyzed BL Lac SED (MAGIC Collaboration 2010)

We have also reconstructed the blazar GLF model based on our modified blazar sequence formulation. We set minimum and maximum gamma-ray luminosities of blazars as 10^{43} erg/s and 10^{50} erg/s in νL_ν at rest-frame 100 MeV as in IT09². Since the modification in SED is mostly in the VHE energy band, the predictions for other wavelength, including the GeV energy band for *Fermi*, hardly change from IT09. For example, the expected *Fermi* blazar count is ~ 720 and ~ 750

¹ NED is operated by the Jet Propulsion Laboratory, California Institute of Technology, under contract with the National Aeronautics and Space Administration.

² Throughout this paper, the blazar luminosity is expressed by isotropic-equivalent luminosity, though blazar emission should be strongly beamed in reality.

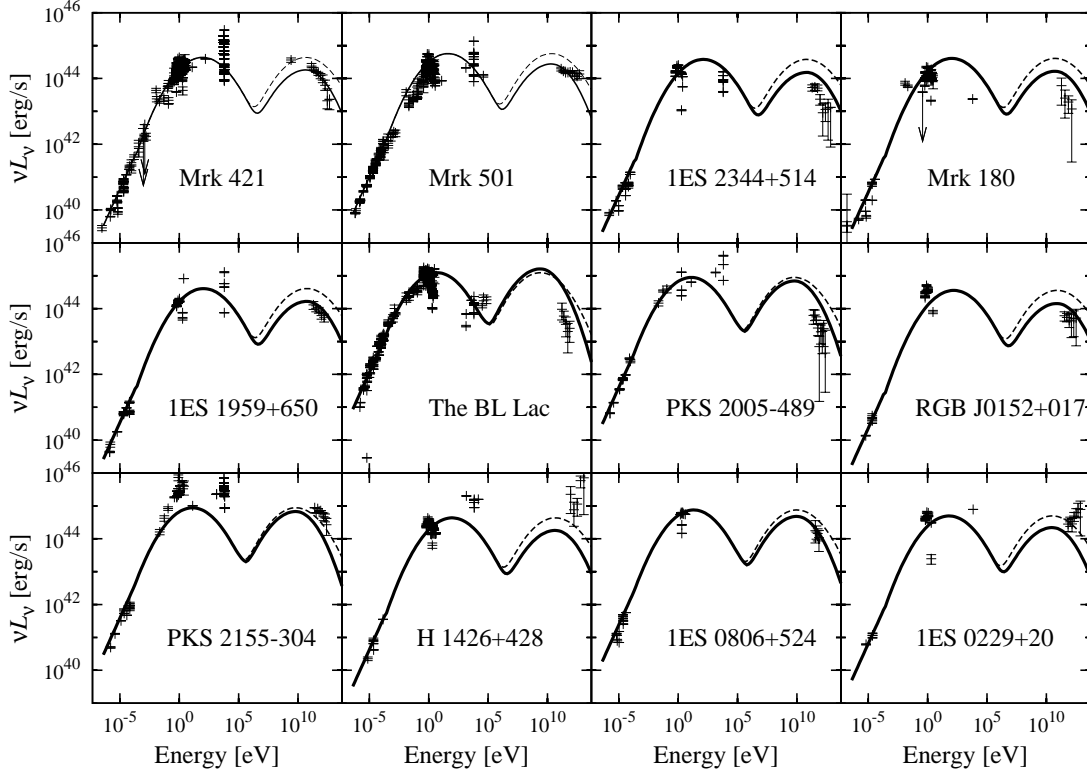


Fig. 1. SEDs (in isotropic equivalent luminosity) of VHE blazars at $z \leq 0.14$. The VHE data points are taken from the literature: Mrk 421(Albert et al. 2007c), Mrk 501(Albert et al. 2007d), 1ES 2344+514(Albert et al. 2007b), Mrk 180(Albert et al. 2006a), 1ES 1959+650 (Albert et al. 2006b), the BL Lac (Albert et al. 2007a), PKS 2005-489 (Aharonian et al. 2005a), RGB J0152+017 (Aharonian et al. 2008), PKS 2155-304 (Aharonian et al. 2005b), 1ES 0806+524 (Acciari et al. 2009), H 1426+428 (Aharonian et al. 2002), and 1ES 0229+200 (Aharonian et al. 2007). Note that VHE data are deabsorbed by the EBL model of Totani & Takeuchi (2002). The data points at energy bands other than VHE are taken from NED. Solid and dashed curves correspond to blazar sequence models by this paper and IT09, respectively.

in the entire sky for our model and IT09, respectively, where we set the *Fermi* sensitivity as 3×10^{-9} photons $\text{cm}^{-2}\text{s}^{-1}$ at >100 MeV corresponding to the 1-year sky survey sensitivity (Atwood et al. 2009). Since *Fermi* 11-months AGN catalog has already detected 596 blazars and 72 unidentified extragalactic gamma-ray sources at high Galactic latitude ($|b| > 10^\circ$), our source count prediction is also consistent with the number of *Fermi* blazars.

The key parameters of the blazar GLF are $(q, \gamma_1, \kappa) = (4.50, 1.10, 1.42 \times 10^{-6})$, where q is the ratio between the bolometric jet luminosity and disk X-ray luminosity, γ_1 the faint-end slope index of GLF, and κ a normalization factor of GLF (see Section. 3 of IT09 for details). Now we can predict the abundance and statistics of blazars in any photon energy bands including VHE gamma-ray.

2.2. EBL models

When we try to make some predictions for extragalactic VHE blazar survey, EBL modeling is crucial. A number of models have been proposed by many authors (e.g. Salamon & Stecker 1998; Totani & Takeuchi 2002; Kneiske, Mannheim, & Hartmann 2002; Kneiske et al. 2004; Primack, Bullock, & Somerville 2005; Stecker, Malkan, & Scully 2006; Mazin & Raue 2007; Raue & Mazin(2008)). Fig. 3 shows optical depth models of Totani & Takeuchi (2002, TT02), Kneiske

et al. (2004, K04), and Raue & Mazin(2008, RM08). Since RM08 constrained EBL optical depth from VHE blazar observations, we present their model below $z = 0.6$. Here we use the optical depth of TT02 as the standard in this paper, because it is in good agreement with RM08 that is consistent with VHE blazar observations at low redshift, and it extends beyond $z \sim 1$ by galaxy evolution modeling that is consistent with galaxy counts and EBL observations in optical and infrared bands (TT02). K04 predicted about twice higher optical depth than TT02, and the expected number of VHE blazars will decrease from our predictions below, when we adopt K04.

3. Predictions for the upcoming CTA era

We consider two modes of future surveys for VHE blazars. One is a blank field sky survey. This is a natural outcome for the nearly all-sky monitoring types of VHE observatories (such as the HAWC and Tibet experiments). For IACTs, various survey designs are possible for a fixed amount of the total observation time, changing the survey area and exposure time for one field of view (FoV) [e.g., the Galactic Plane by H.E.S.S. (Aharonian et al. 2006b)]. The other is follow-up surveys for targets selected at other wavelengths. We particularly consider a follow-up survey of Fermi blazars by CTA.

The sensitivity of VHE detectors is often given in terms of

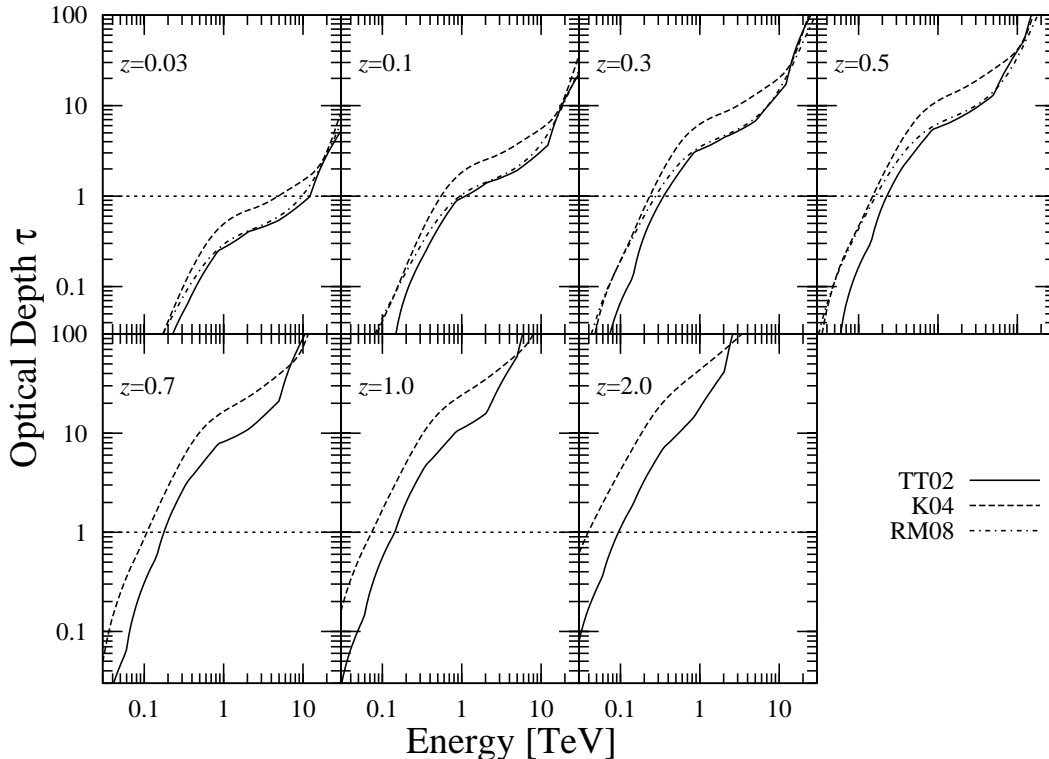


Fig. 3. Optical depth of intergalactic absorption of high energy gamma-rays for various source redshifts as indicated in each panel. Solid, dashed, and dot-dashed curves corresponds to the models of Totani & Takeuchi (2002, TT02), Kneiske et al. (2004, K04), and Raue & Mazin(2008, RM08), respectively. The dotted line marks the level of optical depth $\tau = 1$.

integrated photon flux (total photon flux above a given photon energy). However, a comparison with theoretical prediction is more easily made in terms of energy flux like νF_ν . In this paper, we express the VHE sensitivity in terms of $\nu F_\nu = E^2 dF_\gamma/dE$, where E is the gamma-ray energy and dF_γ/dE the differential photon flux. The sensitivities in integrated photon flux of H.E.S.S., CTA, Tibet-III/MD, and HAWC³ are converted into νF_ν assuming a gamma-ray spectrum of $dF_\gamma/dE \propto E^{-2.5}$, although spectral index varies from source to source in reality. We also assume that the sensitivity limit scales as $\propto T^{-1/2}$, where T is the exposure time. Table 1 summarizes the 5σ CTA sensitivities in several energy bands for some sets of observing time. The sensitivity of CTA will be about one order of magnitude better than that of current IACTs, and the photon energy range will also become about one order of magnitude wider.

3.1. Blank Field Surveys

A blank field survey is the most fundamental mode of observing a sky in a waveband, and free from biases about the pre-selection, except the flux limit of the survey. A catalog of objects obtained by such a survey is important for a statistical study, such as construction of luminosity function. For exam-

Table 1. CTA νF_ν sensitivity in the unit of 10^{-13} erg/cm²/s*.

Energy	Observing time per 1 FoV		
	2 hrs	10 hrs	50 hrs
30 GeV	45	20	9.0
100 GeV	25	11	5.0
300 GeV	5.0	2.2	1.0
1 TeV	3.0	1.3	0.6
10 TeV	10	4.5	2.0

* These sensitivities are converted into νF_ν basis from those in integrated photon flux of 5σ , 50 hrs observation (<http://www.cta-observatory.org/>). Sources are assumed to have a power law differential photon spectrum of $dF_\gamma/dE \propto E^{-2.5}$.

ple, the Galactic plane survey by H.E.S.S. made a breakthrough in the Galactic high energy astronomy by discovering various gamma-ray emitting objects (Aharonian et al. 2006b).

Fig. 4 shows the cumulative source counts per 1 square degree, i.e., the surface number density of blazars brighter than a given threshold flux, predicted by our blazar GLF model in five energy bands of 30 GeV, 100 GeV, 300 GeV, 1 TeV, and 10 TeV as indicated in the panels. The expected counts in the case of no intergalactic absorption are also shown.

First we examine the expected number of blazars detectable by HAWC or Tibet-III/MD experiments. These experiments cover photon energies higher than ~ 1 TeV, and the 1-yr, 5σ sensitivities of these two telescopes are indicated in the 1 and

³ H.E.S.S.: <http://www.mpi-hd.mpg.de/hfm/HESS/>

CTA: <http://www.cta-observatory.org/>

Tibet-III/MD: <http://www.icrr.u-tokyo.ac.jp/em/index.html>

HAWC: <http://hawc.umd.edu/>

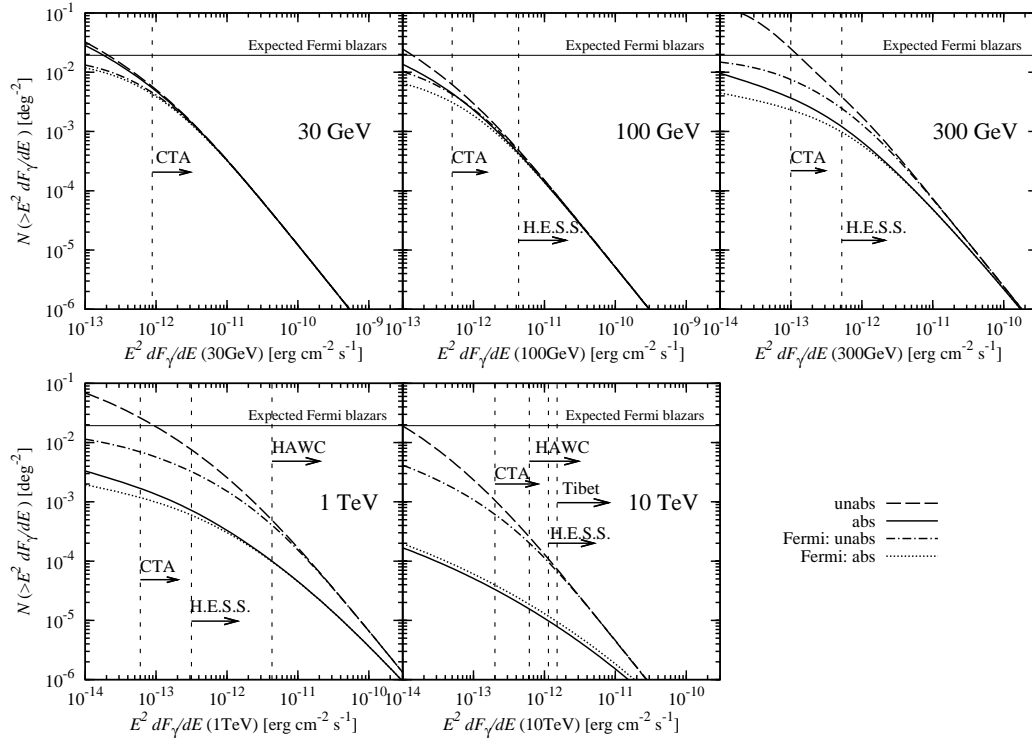


Fig. 4. Cumulative source counts as a function of gamma-ray flux (in νF_ν) of VHE blazars. The five panels correspond to different photon energies as indicated in the panels. The solid curves are predictions by our blazar GLF model. The dotted curves are the same as the solid curves, but for blazars that are detected by Fermi with a sensitivity of $F_{\text{lim}} = 3 \times 10^{-9}$ photons $\text{cm}^{-2} \text{s}^{-1}$ for photon flux above 100 MeV. The intergalactic absorption by EBL is taken into account for the solid and dotted curve, but not in the dashed and dot-dashed curve. The 5- σ detection limits of H.E.S.S. and CTA for 50-hr observation and those of HAWAC and Tibet-III/MD for 1-year observation are also shown. The dotted curve in the panel of 10 TeV is shifted upward artificially by a factor of 1.2 for the purpose of presentation, because the solid and dotted curves totally overlap with each other. The horizontal thin solid line is the total expected number of Fermi blazars with the Fermi sensitivity given above.

10 TeV panels of Fig. 4. The expected number of blazars by a HAWC search at 1 TeV is about four in 4π steradian, and there may be a chance to detect some bright blazars by HAWC. On the other hand, the expected number is less than one at 10 TeV.

Next we consider a blind survey in a fixed survey area A_{survey} by multiple CTA pointing observations. The 50-hr, 5- σ sensitivities of CTA are shown in Fig 4. As an example, we consider a total survey time of $T_{\text{survey}} = 100$ hours, and hence the observation time per field-of-view becomes $T_{\text{FoV}} = T_{\text{survey}}(A_{\text{FoV}}/A_{\text{survey}})$. Here we assume the CTA FoV to be $A_{\text{FoV}} = 20 \text{ deg}^2$ (Aharonian et al. 2006b). Assuming that the flux sensitivity limit simply scales as $\propto T_{\text{FoV}}^{-1/2}$, we find that the expected number of blazars are 0.17, 0.56, 0.89, 2.3, and 3.3 for the assumed survey areas of $A_{\text{survey}} = 40, 200, 400, 2000,$ and 4000 deg^2 , respectively, in the energy band of 300 GeV. The expected numbers in the other energy bands are summarized in Table 2. These results mean that a wider and shallower sky survey is better for a fixed total survey time. However, the expected number of detectable blazars in a blind survey is at most a few in the case of $T_{\text{survey}} = 100$ hrs, which is insufficient for a detailed statistical study such as luminosity function. Typical total observable time for IACTs are 1000 hrs in a year, and a more ambitious survey using $\gtrsim 1000$ hrs may be required to construct a sufficiently large sample. Another important implication is that the contamination of extragalactic objects will be small in the Galactic plane survey by CTA.

It should be kept in mind that there is a considerable uncertainties in the numbers predicted above. The use of the blazar SED sequence is the key to convert the blazar luminosity function in the GeV band into VHE band, but the validity of the blazar sequence is still a matter of debate. Furthermore, VHE SED of our new sequence model is constrained by only 12 VHE blazars. We did not consider the time variability of blazars, because it is difficult to formulate the variability. The luminosity function model parameters have been determined only by about 50 EGRET blazars, but a much larger statistics by *Fermi* will soon allow us a more accurate determination of the parameters of blazar sequence and GLF. Finally, our model includes only known blazar population. A completely different extragalactic population may be found by such a blind survey, which is probably the most exciting possibility and a strong motivation for the survey.

Fig. 5 shows the expected differential redshift distribution for several flux limits. Again, the cases of no intergalactic absorption are also plotted, and the effect of EBL absorption eliminating high redshift blazars is clearly seen. Therefore, the number and highest redshift of VHE blazars would not dramatically increase even with the CTA sensitivity.

3.2. Following up Fermi blazars

Since a blind survey for VHE blazars seems not easy or requiring a large amount of observing time even with the CTA

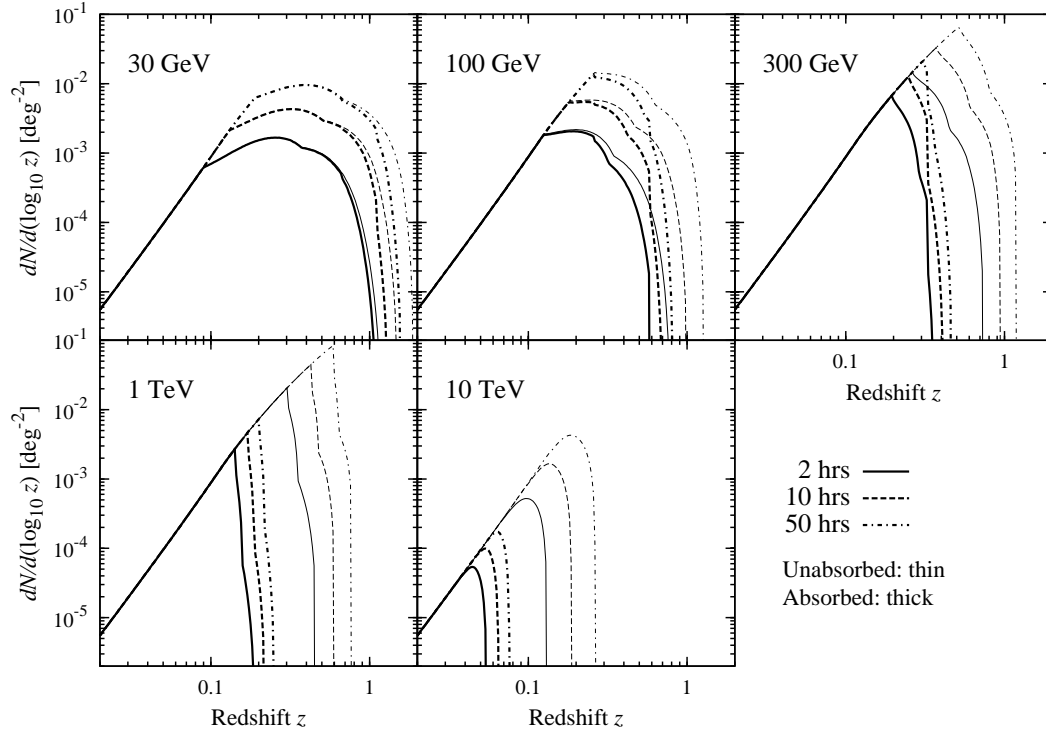


Fig. 5. The differential redshift distribution of VHE blazars in a blind survey down to several values of flux sensitivity. Here, the 5- σ sensitivity is indicated by the corresponding observation time per field (see Table 1 for the sensitivities in physical units). Thick and thin curves are predictions when the intergalactic absorption is taken into account or not, respectively.

Table 2. Expected blazar counts for 100 hours CTA blank field survey

Energy	$A_{\text{survey}} [\text{deg}^2]$				
	40	200	400	2000	4000
30 GeV	0.26	0.59	0.80	1.4	1.7
100 GeV	0.22	0.52	0.72	1.3	1.6
300 GeV	0.17	0.56	0.89	2.3	3.3
1 TeV	0.05	0.14	0.23	0.61	0.92
10 TeV	0.002	0.004	0.007	0.02	0.03

sensitivities, we consider another strategy to find new VHE blazars, i.e., following up blazars detected in other wavelengths. The results of the three-month bright source and 11-month AGN catalog by *Fermi* have already been published (Abdo et al. 2009a, 2009c, 2010), including 596 sources identified as blazars. It is expected that *Fermi* will eventually discover $\gtrsim 1000$ blazars in future survey (Dermer 2007; Inoue & Totani 2009). Very recently Abdo et al. (2009b) have reported that *Fermi* detected GeV gamma-rays from 21 blazars that have been detected in TeV bands. Therefore following up *Fermi* blazars would be one of the most promising ways to increase VHE blazar samples.

Fig. 4 also shows the expected cumulative source counts of blazars that will be detected by *Fermi*, where we set the *Fermi* sensitivity as 3×10^{-9} photons $\text{cm}^{-2}\text{s}^{-1}$ at >100 MeV for one-year survey (Atwood et al. 2009). We adopt this value for *Fermi* sensitivity throughout the paper unless otherwise stated. Taking the sensitivity of 50 hrs observation by CTA (indicated in the figure), the expected number of detectable blazars is not

much different (within a factor of about two) from that of a blind search.

Although ~ 1000 blazars will be detected by *Fermi* in all sky, a simple systematic follow-up of all these blazars will not be practical for CTA. In a realistic future observation, we should set appropriate threshold flux and redshift range of *Fermi* blazars to efficiently select the follow-up targets for CTA. Fig. 6 shows the number of blazars detectable by CTA as a function of *Fermi* GeV flux, for three different sensitivities of CTA observation. This figure tells us that the fraction of *Fermi* blazars detectable by CTA becomes smaller for higher photon energy bands due to sensitivity and intergalactic absorption, indicating that a follow-up survey may become inefficient if only the flux information is utilized.

Since $\sim 70\%$ of *Fermi* blazars have already been measured their redshifts (Abdo et al. 2010), it is expected that a significant fraction of *Fermi* blazars will have their redshift information. Therefore, the redshift information may also be useful to select *Fermi* blazars as the targets for CTA observations, though using redshift information might introduce a further bias in the resulting sample. Fig. 7 shows the region in the *Fermi* flux versus redshift plane for blazars that can be detected by CTA for three different sensitivities. We denote z_τ (depending on observed gamma-ray energy E_γ) as the redshift at which the absorption optical depth becomes $\tau(z_\tau, E_\gamma) = 1$. It should be noted that, even for the same *Fermi* flux, higher- z blazars are more difficult to detect in VHE bands. This is not only by the effect of intergalactic absorption; another effect is that VHE flux becomes relatively smaller compared with the

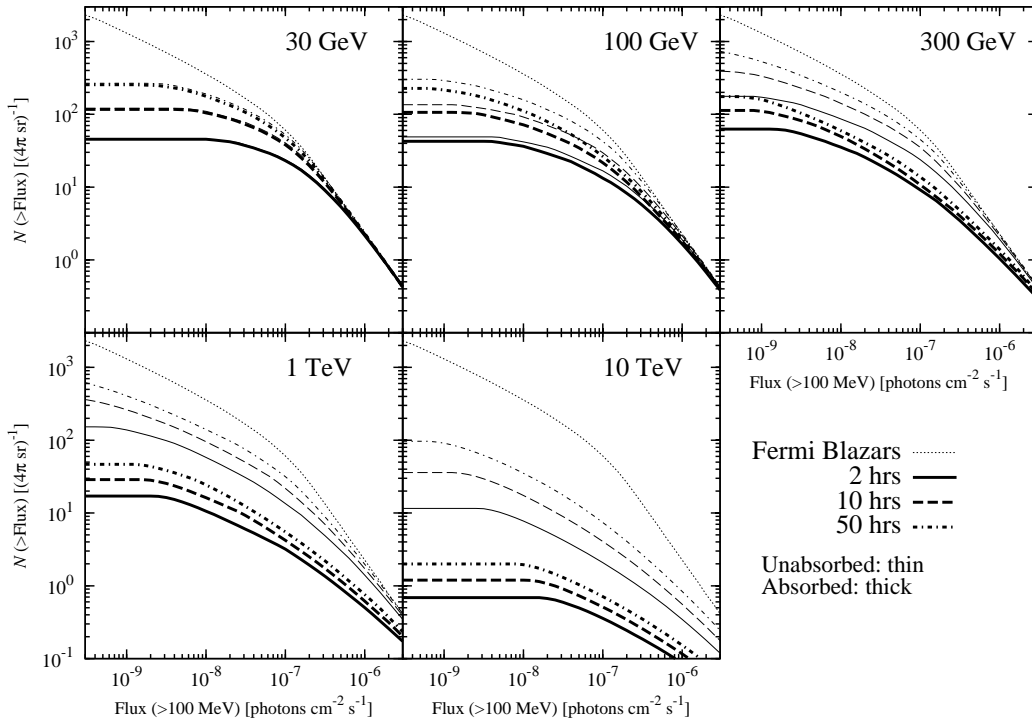


Fig. 6. The source counts of *Fermi* blazars which are detectable by CTA, as a function of flux in the *Fermi* band (>100 MeV). Five panels are for five photon energy bands of CTA, and three different curves are for the different CTA flux sensitivities for each blazar that are the same as those in Fig. 5. See Table 1 for the sensitivity limits in physical units. The dotted curves are for all *Fermi* blazars regardless of the detectability by CTA. Thick curves take into account the intergalactic absorption, while thin curves do not.

Fermi band at larger distances, because of the larger absolute luminosity and the assumed SED sequence. If the SED sequence is valid, one must be careful to discriminate between these two effects in the future analyses.

These two figures will be useful to design the follow-up strategy of *Fermi* blazars by CTA (e.g., the *Fermi* flux and redshift thresholds for CTA targets). The spectral index in the *Fermi* band may also be useful for efficient target selection. A variety of target selection strategies are possible, and the best observing strategy must be determined according to the scientific purposes.

4. On the determination of the EBL

Now we consider to measure EBL by future VHE observations of blazars by CTA, as a particular application of our result. An obvious approach is to use the brightest blazars and measure their VHE spectra precisely, to measure the intergalactic absorption feature and hence EBL. The improved CTA sensitivity would allow us to measure the absorption features in a wider range of photon energy, and correspondingly, redshift. The optical depth to a source at a redshift z is an integration of EBL from redshift zero to z along the photon path, and the optical depth is mainly contributed by EBL photons whose frequency satisfies the relation $E_\gamma h\nu_{\text{EBL}} \sim 2(m_e c^2)^2$. Therefore EBL measurements by blazars having a variety of redshifts would give us information about evolution of EBL as well as spectrum.

Another possible approach to measure EBL is using a break in redshift distribution by intergalactic absorption. Although this approach would require a larger sample than using a single VHE spectrum of bright blazars, the uncertainty concerning the intrinsic spectrum could be minimized by looking a statistical signature in redshift distribution. Here we quantitatively discuss the feasibilities of these two approaches, which are expected to be complementary to each other.

4.1. Absorption Features in Brightest Blazar Spectra

Fig. 8 shows blazar source counts as a function of VHE flux around z_τ in the entire sky for the four energies of 100 GeV, 300 GeV, 1 TeV, and 10 TeV, in the case of following up *Fermi* blazars with the intergalactic absorption taken into account. The values of z_τ are 1.5, 0.36, 0.10, and 0.035 for each energy, respectively. The flux of the brightest blazars available at the four photon energy bands are $\sim 2, 20, 100,$ and $3 \times 10^{-13} \text{ erg cm}^{-2} \text{ s}^{-1}$ (the fluxes at which the expected number becomes order unity in this figure).

First we set the required signal-to-noise to be 5σ per logarithmic energy bin width of $\Delta E/E = 1$ to detect absorption feature. This corresponds to 7.2σ detection for integrated flux. From the estimates of brightest blazar flux, the required observing time to achieve this S/N is 450, 0.36, 0.003, and 40 hours for the four energy bands, respectively. The photon energy resolution of CTA may become as good as $\Delta E/E$ to be 0.1, and if we require $S/N = 5$ per this spectral resolution, the required significance for integrated flux becomes 19σ . Then

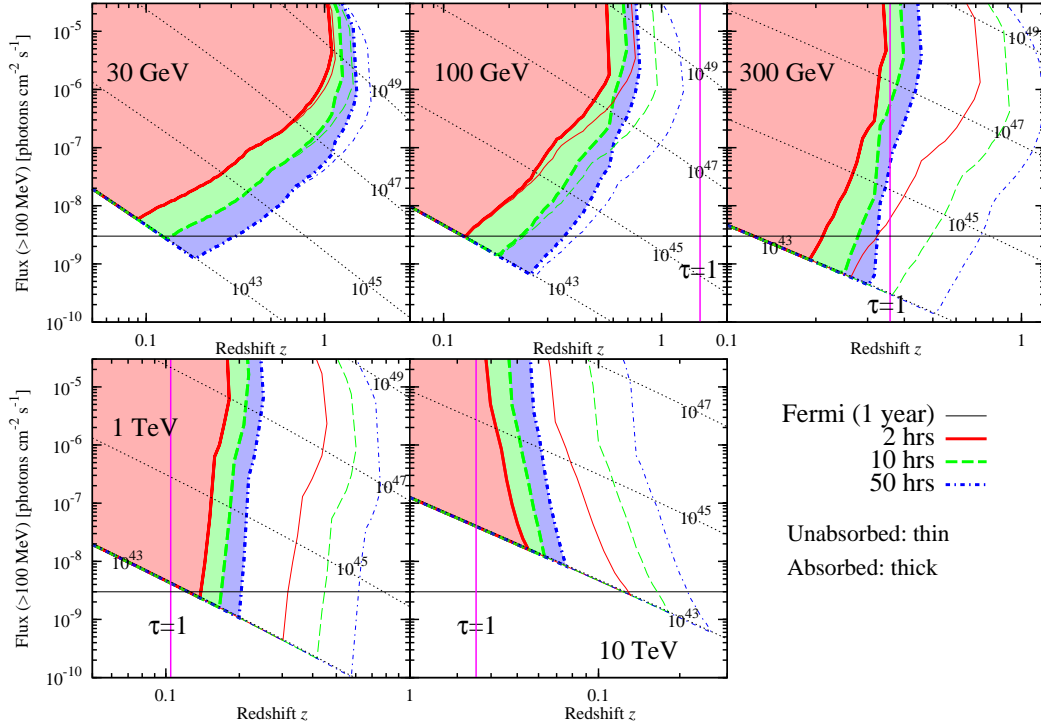


Fig. 7. The region of *Fermi* blazars that can be detected by CTA, in Fermi photon flux and redshift plane. The five panels correspond to different photon energy bands of CTA, as indicated in the panels. Different colors correspond to different CTA flux thresholds that are the same as those in Figs. 5 and 6. The regions detectable are shaded by the corresponding colors. The horizontal black solid line shows 1-year Fermi sensitivity, and the vertical magenta solid line is the redshift at which the optical depth of intergalactic absorption becomes unity, i.e. $\tau(z_\tau) = 1$. Dotted black lines are contours of gamma-ray luminosities (νL_ν at restframe 100 MeV) of blazars in units of [erg/s] as indicated in panels.

the required observing time becomes 3000, 2.4, 0.02, and 270 hours for the four energy bands, respectively. These results indicate that we will have bright blazars at various redshift range of 0.01–1.5 to measure EBL with a reasonable amount of observing time. Especially, we will be able to obtain high resolution spectra of bright blazars with reasonable observing time between 0.3–1 TeV (corresponding to $z = 0.10$ –0.36).

4.2. Cut-offs in Redshift Distributions

Next we consider the break signature in redshift distribution. Here we suppose that redshifts of the majority of Fermi blazars are already known at the time of future VHE observation, which seems a reasonable assumption as discussed in the previous section. Suppose a VHE photon energy E_γ and corresponding z_τ . We expect a strong break around z_τ in the redshift distribution of Fermi blazars that are detectable by the VHE photon energy band around E_γ , and such a break should give a strong constraint on EBL. Such a break is demonstrated in Fig. 9, where we show the redshift distribution of Fermi blazars whose Fermi flux is brighter than $F(> 100\text{MeV}) = 3 \times 10^{-9}$ photons $\text{cm}^{-2} \text{s}^{-1}$ and which are detectable at 300 GeV band with several different CTA sensitivities. Most of Fermi blazars at $z \lesssim 0.3$ can be detected by CTA, while sharp cut-offs appear as expected, at redshifts significantly lower than the cases ignoring intergalactic absorption.

The key question for this approach is whether there are a sufficient number of blazars to construct a statistically large

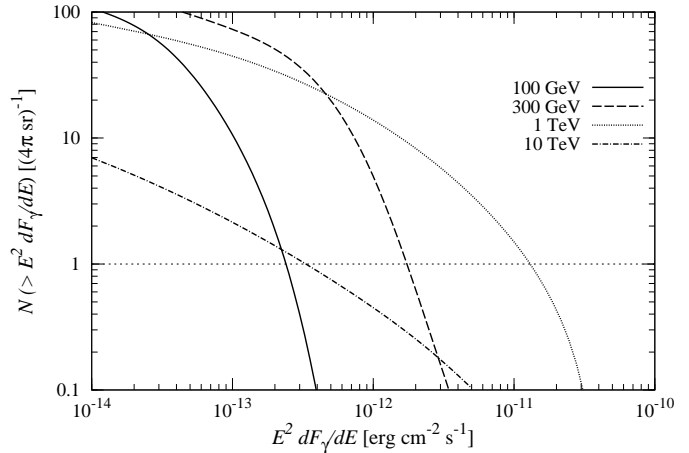


Fig. 8. Source counts of VHE blazars as a function of VHE flux in the four energy bands indicated in the figure, assuming a follow-up of *Fermi* blazars down to the flux threshold of $F(> 100\text{MeV}) = 3 \times 10^{-9}$ photons $\text{cm}^{-2} \text{s}^{-1}$. Here, the redshift range is limited around the expected break by EBL absorption: $z_\tau/2 < z < 2 \times z_\tau$. The intergalactic absorption is taken into account. Horizontal dotted line marks the level of one blazar in the entire sky.

enough sample to see the break. This available number should change with the supposed redshift (or VHE photon energy). Fig. 10 gives an answer to this question; it shows blazar counts as a function of Fermi flux, for Fermi blazars around $z \sim z_\tau$ in three VHE photon energy bands. In this figure, we show source counts of blazars that can be detected with several different CTA sensitivities, as well as the original Fermi source counts. Then we can estimate the number of targets to be observed and detection rate at VHE bands for a given Fermi threshold flux and VHE sensitivities. We did not show panels for 30 and 100 GeV because the expected break redshift by intergalactic absorption is comparable with or larger than the redshift limit coming from CTA sensitivity with a reasonable amount of observing time (see Fig. 7).

From this result, it seems difficult to construct a statistically large ($\gtrsim 10$) sample at 10 TeV. However, in the 300 GeV and 1 TeV bands, we will be able to construct a sample of a few tens of blazars with 50 and 30 hrs of total observational time by following up Fermi blazars down to $F(> 100\text{MeV}) = 3 \times 10^{-9}$ photons $\text{cm}^{-2} \text{s}^{-1}$, respectively. Here we assumed that all samples are 5σ detection in integral flux and the minimum observational time for each blazar is 0.5 hrs. If we require 10σ detection for each blazar at these VHE sensitivities, the total observation time necessary for this survey becomes 200 and 100 hrs, respectively. Therefore, this statistical approach seems feasible in the VHE energy range of 0.3–1 TeV, which is complementary to EBL measurements using spectral break of bright blazars.

It should be noted that the location and shape of the break in the redshift distribution depends not only on EBL but also VHE luminosity function of blazars, which may induce some systematic uncertainties in the EBL measurement by this approach. However, we should be able to construct luminosity distribution of VHE blazars that is not affected by intergalactic absorption by using blazars slightly below z_τ . We do not expect a strong cosmological evolution of VHE luminosity function of blazars in a small range of redshift around z_τ , and we can apply the VHE luminosity distribution below z_τ to derive the optical depth of intergalactic absorption, without invoking uncertain theoretical modeling.

5. Summary

In this paper, we estimated the expected source counts and redshift distribution of VHE blazars for the next generation IACTs such as CTA and AGIS missions based on the latest blazar GLF model of Inoue & Totani (2009). For this purpose, we developed a new SED sequence formula of blazars taking into account the latest VHE data, while the previous sequence formulae were constructed using only data at photon energies below the EGRET/Fermi energy band. The parameters of our blazar GLF are also refined with this new SED formula, by fitting to the GeV blazar data. Our modeling does not include time variabilities of VHE blazars, and blazars at flaring states would be more easily detected than estimated here.

We made predictions for future VHE blazar survey in two observing modes: one is a blind survey in a blank field, and another is a following up survey of *Fermi* blazars. We found that CTA will detect a few VHE blazars by a blind survey using a

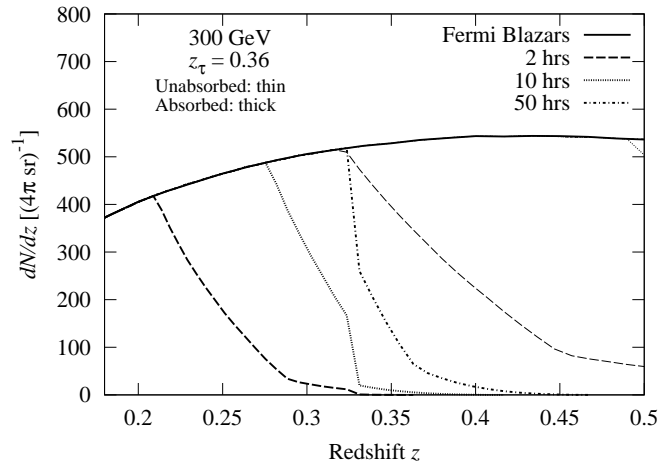


Fig. 9. The redshift distribution of blazars detectable in the 300 GeV band, for the case of following up *Fermi* blazars down to the Fermi flux threshold of $F(> 100\text{MeV}) = 3 \times 10^{-9}$ photons $\text{cm}^{-2} \text{s}^{-1}$. Different three curves are for different CTA sensitivity limits as indicated in the figure in terms of the exposure time. (See Table 1 for the sensitivity flux in physical units.) Thin and thick curves correspond to unabsorbed cases and absorbed cases, respectively. Redshift distribution of *Fermi* blazars is also shown as black solid line.

total survey time of 100 hours. Therefore a large amount of observing time ($\gtrsim 1000$ hrs) is required to construct a statistically large sample of blazars selected only by VHE bands. However, this suggests that blazar contamination in the Galactic plane survey should not be significant even in the era of the next generation IACTs. We also found that future all sky gamma-ray detectors such as HAWC and Tibet-III/MD, will detect only a few VHE blazars in one year survey in the entire sky. The survey design for a follow-up survey of Fermi blazars should be dependent on the scientific purposes. Here we presented a plot for regions in the Fermi flux versus redshift plane where the Fermi blazars can be detected by VHE observations for several different sensitivities.

As a particular example of Fermi blazar follow-up surveys, we considered a survey for the purpose of determination of EBL by VHE observation. CTA can observe VHE blazars that are sufficiently bright to get detailed spectra with high S/N in the redshift range of $z \sim 0.10$ – 0.36 , corresponding to the absorption cut-off energy 1–0.3 TeV, and hence we can constrain not only EBL flux but also its spectra and/or redshift evolution. It will also be possible to construct a statistically large sample ($\gtrsim 30$) of blazars at $z \sim 0.10$ – 0.36 to constrain EBL by the sharp break in the redshift distribution. This approach could avoid or minimize the uncertainty about intrinsic blazar spectra, and hence could be complementary to using a few spectra of brightest blazars.

This research has made use of the NASA/IPAC Extragalactic Database (NED) which is operated by the Jet Propulsion Laboratory, California Institute of Technology, under contract with the National Aeronautics and Space Administration. This work was supported by the Grant-in-Aid for the Global COE Program "The Next Generation of Physics, Spun from Universality and Emergence" from the Ministry of Education,

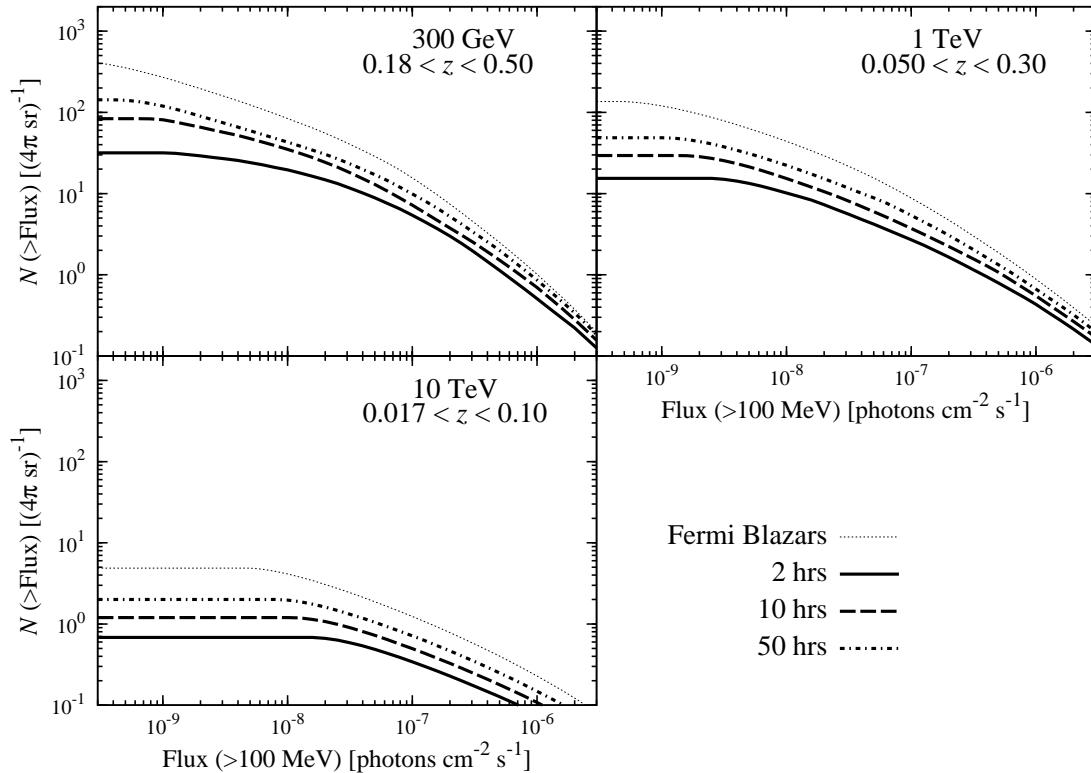


Fig. 10. Source counts of Fermi blazars as a function of Fermi-band flux, within limited redshift ranges around the expected redshift break by EBL absorption. Different panels are for different VHE photon energy bands, and three different curves in each panel are for those detectable by the VHE band with the CTA exposure time indicated in the figure. See Table 1 for the corresponding VHE flux sensitivity in physical units. The dotted line is the original Fermi source counts regardless of the detectability in VHE bands.

Culture, Sports, Science and Technology (MEXT) of Japan. YI acknowledges support by the Research Fellowship of the Japan Society for the Promotion of Science (JSPS).

Appendix 1. The New Blazar SED Sequence Templates

We introduce some modifications on the inverse Compton (IC) component of the blazar SED sequence model of IT09 to make it in better agreement with VHE blazars data. We define $\psi(x) \equiv \log_{10}[\nu L_\nu / (\text{erg s}^{-1})]$ with $x \equiv \log_{10}(\nu/\text{Hz})$ (ν in rest-frame). The empirical SED sequence model of blazars is the sum of the synchrotron $[\psi_s(x)]$ and IC $[\psi_c(x)]$ emissions. Each component is described by a combination of a linear and a parabolic function at low and high photon frequencies, respectively. We take $\psi_R \equiv \log_{10}[L_R / (\text{erg s}^{-1})]$ as a reference of a blazar luminosity, where L_R is νL_ν luminosity in the radio band ($\nu_R = 5$ GHz or $x_R = 9.698$).

Here we only describe the modified points from the IT09 blazar sequence model. The peak frequency of IC component ν_c is determined by the relation to that of the synchrotron component, ν_s , where ν_s has been determined as a function of ψ_R as in IT09. This relation has been changed into the following equation:

$$\nu_c/\nu_s = \begin{cases} 5 \times 10^8 & (\psi_R < 43.0) \\ 5 \times 10^8 [10^{(\psi_R - 43.0)}]^{-0.1} & (\psi_R \geq 43.0) \end{cases}, \quad (\text{A1})$$

instead of the fixed value $\nu_c/\nu_s = 5 \times 10^8$ used by IT09. The

parabolic part of the IC component, ψ_{c2} is modified as follows:

$$\psi_{c2}(x) \equiv \begin{cases} -[(x - x_c)/\sigma]^2 + \psi_{c,p} & (x < x_c) \\ -1.5[(x - x_c)/\sigma]^2 + \psi_{c,p} & (x \geq x_c) \end{cases}, \quad (\text{A2})$$

from eq. A6 of IT09. Note that the shape of the parabolic part is now different for the synchrotron and IC components. Such a difference is possible by several effects, e.g., external photon field for target photons of IC, internal absorption of high-energy gamma-rays by pair production, or the Klein-Nishina effect. Finally, the peak luminosity of the IC component, $\psi_{c,p}$, is changed into the following form:

$$\psi_{c,p} = -0.014(\psi_R - 36.2)(\psi_R - 44.6)(\psi_R - 55.0) + 47.7. \quad (\text{A3})$$

from eq. A13 of IT09.

Fig. 11 shows the blazar sequence SED of IT09 and of this paper.

References

- Abdo, A. A. et al. 2009a, ApJ, 700, 597
- . 2009b, ApJ, 707, 1310
- . 2009c, ApJS, 183, 46
- . 2010, arXiv:1002.0150
- Acciari, V. et al. 2009, ApJL, 690, L126
- Aharonian, F. et al. 2002, A&A, 384, L23
- . 2005a, A&A, 436, L17
- . 2005b, A&A, 430, 865

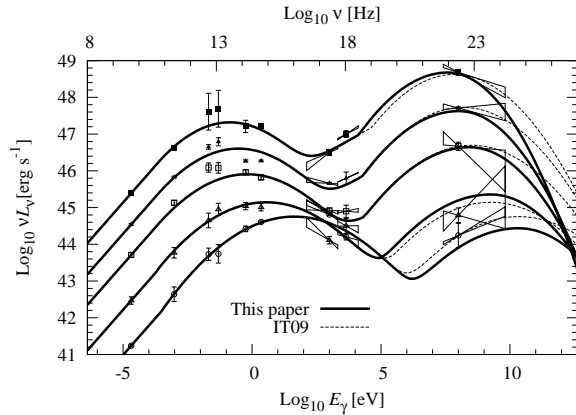


Fig. 11. The blazar SED sequence. The data points are the average SED of the blazars studied by Fossati et al. (1998) and Donato et al. (2001). The solid and dashed curves are the empirical SED sequence models of this paper and IT09, respectively.

—. 2006a, *Nature*, 440, 1018
 —. 2006b, *ApJ*, 636, 777
 —. 2007, *A&A*, 475, L9
 —. 2008, *A&A*, 481, L103
 Albert, J. et al. 2006a, *ApJL*, 648, L105
 —. 2006b, *ApJ*, 639, 761
 —. 2007a, *ApJL*, 666, L17
 —. 2007b, *ApJ*, 662, 892
 —. 2007c, *ApJ*, 663, 125
 —. 2007d, *ApJ*, 669, 862
 Atwood, W. B. et al. 2009, *ApJ*, 697, 1071
 Chiang, J., Fichtel, C. E., von Montigny, C., Nolan, P. L., & Petrosian, V. 1995, *ApJ*, 452, 156
 Chiang, J. & Mukherjee, R. 1998, *ApJ*, 496, 752
 de Angelis, A., Mansutti, O., & Persic, M. 2008, *Nuovo Cimento Rivista Serie*, 31, 187
 Dermer, C. D. 2007, *ApJ*, 659, 958
 Donato, D., Ghisellini, G., Tagliaferri, G., & Fossati, G. 2001, *A&A*, 375, 739
 Fermi-LAT collaboration 2010, arXiv:1002.3603
 Fossati, G., Celotti, A., Ghisellini, G., & Maraschi, L. 1997, *MNRAS*, 289, 136
 Fossati, G., Maraschi, L., Celotti, A., Comastri, A., & Ghisellini, G. 1998, *MNRAS*, 299, 433
 Ghisellini, G., Maraschi, L., & Tavecchio, F. 2009, *MNRAS*, 396, L105
 Gould, R. J. & Schröder, G. 1966, *Physical Review Letters*, 16, 252
 Hartman, R. C. et al. 1999, *ApJS*, 123, 79
 Hasinger, G., Miyaji, T., & Schmidt, M. 2005, *A&A*, 441, 417
 Hauser, M. G. & Dwek, E. 2001, *ARA&A*, 39, 249
 Inoue, Y. & Totani, T. 2009, *ApJ*, 702, 523
 Inoue, Y., Totani, T., Inoue, S., Kobayashi, M. A. R., Kataoka, J., & Sato, R. 2010, arXiv:1001.0103
 Inoue, Y., Totani, T., & Ueda, Y. 2008, *ApJL*, 672, L5
 Jelley, J. V. 1966, *Physical Review Letters*, 16, 479
 Kneiske, T. M., Bretz, T., Mannheim, K., & Hartmann, D. H. 2004, *A&A*, 413, 807
 Kneiske, T. M., Mannheim, K., & Hartmann, D. H. 2002, *A&A*, 386, 1
 Kubo, H., Takahashi, T., Madejski, G., Tashiro, M., Makino, F., Inoue, S., & Takahara, F. 1998, *ApJ*, 504, 693
 MAGIC Collaboration, Albert, J., et al. 2008, *Science*, 320, 1752

MAGIC Collaboration 2010, arXiv:1002.2951
 Mazin, D. & Raue, M. 2007, *A&A*, 471, 439
 Mori, M. 2009, *Journal of the Physical Society of Japan*, 78SA, 78
 Mücke, A. & Pohl, M. 2000, *MNRAS*, 312, 177
 Narumoto, T. & Totani, T. 2006, *ApJ*, 643, 81
 Padovani, P., Ghisellini, G., Fabian, A. C., & Celotti, A. 1993, *MNRAS*, 260, L21
 Padovani, P., Giommi, P., Landt, H., & Perlman, E. S. 2007, *ApJ*, 662, 182
 Primack, J. R., Bullock, J. S., & Somerville, R. S. 2005, in *American Institute of Physics Conference Series*, Vol. 745, *High Energy Gamma-Ray Astronomy*, ed. F. A. Aharonian, H. J. Völk, & D. Horns, 23–33
 Raue, M., & Mazin, D. 2008, *International Journal of Modern Physics D*, 17, 1515
 Salamon, M. H. & Stecker, F. W. 1994, *ApJL*, 430, L21
 —. 1998, *ApJ*, 493, 547
 Stecker, F. W., Malkan, M. A., & Scully, S. T. 2006, *ApJ*, 648, 774
 Stecker, F. W. & Salamon, M. H. 1996, *ApJ*, 464, 600
 Stecker, F. W., Salamon, M. H., & Malkan, M. A. 1993, *ApJL*, 410, L71
 Totani, T. & Takeuchi, T. T. 2002, *ApJ*, 570, 470
 Ueda, Y., Akiyama, M., Ohta, K., & Miyaji, T. 2003, *ApJ*, 598, 886